

Available online at [www.sciencedirect.com](http://www.sciencedirect.com)

SCIENCE @ DIRECT®

Molecular Aspects of Medicine xxx (2006) xxx–xxx

MOLECULAR  
ASPECTS OF  
MEDICINE[www.elsevier.com/locate/mam](http://www.elsevier.com/locate/mam)

Review

## LightUp<sup>®</sup> probes in clinical diagnostics

Mikael Leijon<sup>a,\*</sup>, Mehrdad Mousavi-Jazi<sup>a</sup>, Mikael Kubista<sup>b</sup><sup>a</sup> *LightUp Technologies AB, Lunastigen 5, SE-141 44 Huddinge, Sweden*<sup>b</sup> *Department of Chemistry and Biosciences, Molecular Biotechnology,  
Chalmers University of Technology and TATAA Biocenter, Lundberg Laboratory,  
40530 Göteborg, Sweden*

---

### Abstract

The LightUp<sup>®</sup> Probe technology has now matured and reached the phase where it has been implemented in commercial reagent kits, i.e. the ReSSQ<sup>®</sup> product line. Several properties of the LightUp<sup>®</sup> probes make them particularly suitable for clinical settings. For instance, extraordinary shelf life and a chemical stability that allows convenient fridge storage. The origin of the higher stability of LightUp<sup>®</sup> probe kits compared to others, based on alternative probe technologies, is partly the relatively good stability of cyanine dyes but also the resistance towards nucleases and proteases of the synthetic DNA analogue peptide nucleic acid that is used as the sequence recognizing element in LightUp probes. It is clear from recent trends in the PCR amplification hardware technology that the instrumentation is becoming more flexible and less adapted for dedicated probe chemistries. This will pave the way for increased standardization in the field of DNA diagnostics and the development of cross-platform assays.

In the present review the LightUp technology will briefly be presented and discussed. The utility of the technology will be illustrated by examples from cytomegalovirus quantification and monitoring of the viral load of the SARS Coronavirus. An example of cancer diagnostics by detection of altered gene expression patterns will also be shown.

© 2006 Elsevier Ltd. All rights reserved.

*Keywords:* Quantitative PCR; Real-time detection; Fluorescent probes; Peptide nucleic acid; Asymmetric cyanine dyes; Viral diagnostics; Viral load; LightUp<sup>®</sup> probes

---

\* Corresponding author.

**Contents**

1. Introduction . . . . .	00
2. The LightUp <sup>®</sup> probe . . . . .	00
3. Diagnosing cytomegalovirus with LightUp <sup>®</sup> probes . . . . .	00
4. Diagnosing SARS coronavirus with LightUp <sup>®</sup> probes. . . . .	00
5. Diagnosing lymphoma with LightUp <sup>®</sup> probes . . . . .	00
5.1. Sample preparation . . . . .	00
5.2. RNA extraction and cDNA analysis . . . . .	00
5.3. LightUp <sup>®</sup> probes and PCR . . . . .	00
5.4. Classification of patient samples . . . . .	00
6. Conclusions. . . . .	00
References . . . . .	00

---

**1. Introduction**

The use of real-time PCR in molecular diagnostics has rapidly gained ground and has become the golden standard in many instances, in particular when sensitivity is a concern and quantification is desired, for example, when monitoring the effect of anti-viral treatment (Mackay et al., 2002; Mackay, 2004; Mengoli et al., 2004; Tanaka-Kitajima et al., 2005). An additional advantage is that the detection takes place in a homogeneous closed-tube format, which means a significantly reduced risk for carry-over contamination compared to conventional methods (Foy and Parkes, 2001). PCR-based assays are particularly sensitive and robust for detection and quantification of DNA viruses, due to the high conservation of the genomic materials over different strains in combination with the high chemical stability of deoxyribonucleic acids. The remarkable sensitivity of PCR, where a single DNA copy can be detected by an optimized assay, makes the extraction procedure the limiting factor in the diagnostic setting rather than the PCR-coupled detection step (Fafi-Kremer et al., 2004; Schuurman et al., 2005; Uhl et al., 2005). However, even if nucleic acid extraction has been successful there are several ways by which the PCR amplification/detection step may fail. Among these are: (i) the target for primers and/or probe may not be conserved (particularly relevant in infectious disease diagnostics) (Herrmann et al., 2004; Nye et al., 2005), (ii) the fluorescent probes used in real-time PCR are frequently chemically unstable and may be degraded.

**2. The LightUp<sup>®</sup> probe**

Recently, the LightUp<sup>®</sup> probe was constructed to alleviate these drawbacks encountered in PCR based diagnostics (Svanvik et al., 2000a,b; Leijon, 2004). This is accomplished by the use of a fluorescent reporter dye that is coupled to an oligomer of the DNA analogue peptide nucleic acid (PNA) by a flexible linker (Fig. 1).

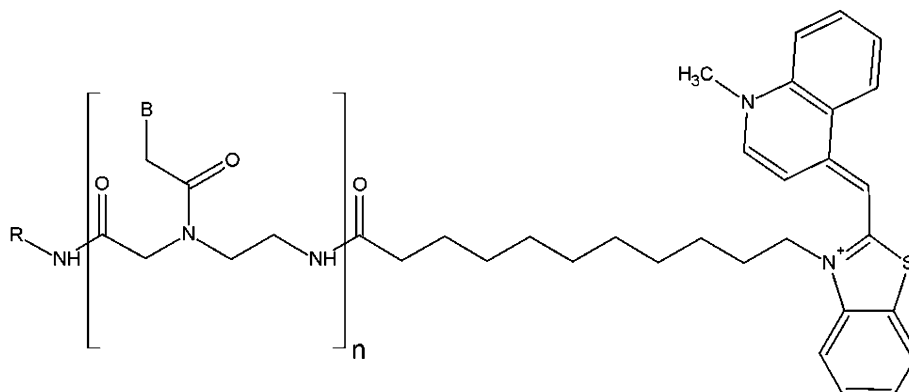


Fig. 1. A LightUp<sup>®</sup> probe with Thiazole Orange (TO) as the fluorescent dye.

PNA is an uncharged isomorphous DNA mimic composed of *N*-(2-aminoethyl)glycine subunits (Nielsen et al., 1991) that provides strong but still specific binding and serves as the sequence recognizing element of the probe. In fact, PNA has the remarkable property of exhibiting higher sequence specificity, in terms of melting point decrease, when bound to DNA than DNA itself (Egholm et al., 1993). Shorter probes can be used with the LightUp<sup>®</sup> Probe technology than with most competing DNA based probe technologies (Livak et al., 1995; Tyagi and Kramer, 1996; Bernard et al., 1998; Mackay et al., 2002). This is due to the high binding affinity of PNA that is further augmented by the dye interaction with DNA. Thus, conserved patches can be found more easily in highly varying microbial or viral genomes. In this respect LightUp probes resemble TaqMan<sup>®</sup> minor groove binding (MGB) probes (Afonina et al., 1997). The fluorophore used in LightUp<sup>®</sup> probes is an asymmetric cyanine dye that fluoresces when the probe binds its target DNA but is virtually non-fluorescent when the probe is free in solution. One example is thiazole orange shown in Fig. 1. Other examples are the SYBR Green proprietary dye from Molecular probes Inc (Oregon, USA), and the BOXTO dye (Karlsson et al., 2003, 2004) that is shown in Fig. 2. The use of PNA is important. Since the dye is positively charged, a significantly higher background signal would result from internal binding of the dye if DNA was used instead of PNA (Svanvik et al., 2001). This class of fluorescent dyes are also relatively stable and the ReSSQ<sup>®</sup> kits that are based on the

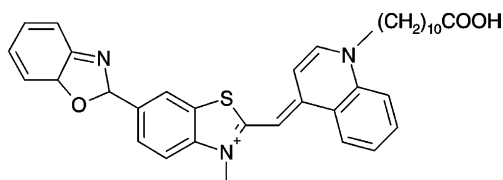


Fig. 2. Structure of the BOXTO dye.

LightUp<sup>®</sup> probe can be stored in the fridge rather than the freezer storage typical for other PCR kits. These dyes in combination with the PNA backbone, which is degraded by neither nucleases nor proteases (Demidov et al., 1994), amounts to very stable probes and robust assays. To further improve the stability of the ReSSQ<sup>®</sup> product line the nucleic acids standard materials are provided lyophilized.

DNA based sequence recognizing fluorescent probes usually utilize fluorophore quencher pairs that are separated during the amplification process. TaqMan<sup>®</sup> probes are degraded by the 5'-nuclease activity of the DNA polymerase which releases the fluorophore from its sequence recognizing element, and thereby separates it from the quencher so that fluorescence emission can occur (Livak et al., 1995). Molecular Beacons achieve the same goal by a rearrangement of the secondary structure upon hybridization, which causes a separation of the quencher and the fluorophore (Tyagi and Kramer, 1996). Fluorescence resonance energy transfer (FRET) probes work slightly differently. Instead of the acceptor dye functioning as a quencher, it emits the detectable fluorescence when the two probes bind adjacent to each other on the target DNA molecule (Bernard et al., 1998). The LightUp<sup>®</sup> Probe works by a different mechanism. The probe has only a single asymmetric cyanine dye. This type of dye releases the excitation energy by internal motion when free in solution and is under these conditions virtually non-fluorescent and hence it is self-quenched. When bound to DNA, however, the dye becomes brightly fluorescent due to motional hindrance in the bound state (Svanvik et al., 2000a).

### **3. Diagnosing cytomegalovirus with LightUp<sup>®</sup> probes**

Immunosuppressed transplant recipients as well as persons infected with human immunodeficiency virus type 1 (HIV-1) are susceptible to severe cytomegalovirus (CMV) infections. Furthermore, congenital CMV infection with high morbidity rate is common. It is therefore important to detect this condition in clinical practice.

In transplant recipients, CMV load is used as an indicator of active CMV disease and for monitoring the effect of anti-viral treatment (Mengoli et al., 2004; Kalpoe et al., 2005; Tanaka-Kitajima et al., 2005). In HIV patients, the risk of developing CMV disease has been reported to be directly related to the quantity of CMV in the plasma (Spector et al., 1998, 1999).

Several commercial tests are available, e. g. the COBAS AMPLICOR<sup>®</sup> CMV MONITOR Test (Roche Diagnostics), the Hybrid Capture<sup>®</sup> System CMV DNA test (Digene Corp.) and the NucliSens<sup>®</sup> CMV pp67 assay (bioMérieux). Although all these tests are very useful, in-house so-called home-brew real-time PCR assays have come to increasing use. The main reasons are the superior sensitivity of PCR, the closed tube format of real-time PCR, which minimizes the risk for cross-over contamination, and the possibility of reproducible and precise viral load quantifications, as outlined above. However, the results from home-brew assays are often not reproducible between laboratories and there is consequently a need for standardization.

The ReSSQ<sup>®</sup> Assays (LightUp Technologies, Huddinge, Sweden) is a new line of commercial kits for qualitative and quantitative detection of viral DNA in clinical

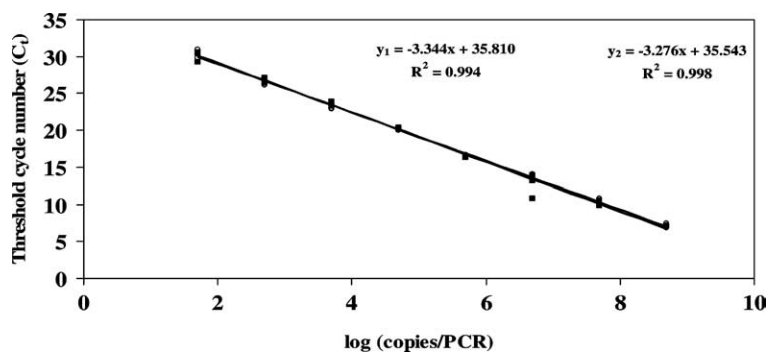


Fig. 3. Dynamic range of the ReSSQ<sup>®</sup> CMV Assay. Serial dilutions of CMV DNA were analyzed in quadruplicates and the threshold cycle number ( $C_t$ ) was plotted against the log CMV DNA copy number. Values from two separate experiments, indicated as gray and black boxes and lines respectively. The regression line was obtained by least-square fitting.

samples that tries to bridge this gap and provide a standardized test built on the LightUp<sup>®</sup> probe technology. In real-time PCR applications quantification is obtained by comparing the PCR cycle at which the fluorescence reaches a certain threshold level for the unknown clinical sample with the PCR threshold cycles values from a sequential (usually 10 fold) dilution series of the standard DNA. In Fig. 3 the dynamic range and reproducibility of the ReSSQ<sup>®</sup> CMV Assay is illustrated from the standard curve obtained in quadruplicates and repeated in two runs. The slopes of  $-3.344$  and  $-3.276$  corresponds to essentially 100% PCR reaction efficiency ( $-3.322$ ). The standard curves are perfectly linear in standard curve interval of  $10^2$ – $10^9$  copies/PCR (Zweyberg Wirgart et al., 2005).

The Quality Control for Molecular diagnostics (QCMD) initiative (Wallace, 2003) serves to provide a reference for comparison between different diagnostics labs as well as commercial kit manufacturers. To this end QCMD designs and develops quality control materials and proficiency programmes. In Table 1 (reproduced from Zweyberg Wirgart et al., 2005) the quantification of the QCMD CMV proficiency panels of 2002 and 2003 obtain by using the ReSSQ<sup>®</sup> CMV assay are shown. The viral loads measured by the ReSSQ<sup>®</sup> assay are close to the QCMD target values on both panels with an average deviation of only 23%. Furthermore, all negative controls are confirmed without false-positive results. Zweyberg Wirgart and colleagues did also use the ReSSQ<sup>®</sup> assay to monitor the effect of anti-varial treatment and compared the results with those obtained with the AMPLICOR CMV MONITOR assay (Roche Diagnostics). The CMV DNA load was monitored in one allogeneic bone marrow-transplanted patient during a period of 175 days (Fig. 4). After 2 months of prophylactic Valtrex therapy with very low or undetectable CMV DNA levels, the viral load increased significantly at day 65 and continued to rise, as determined by both assays. The patient was therefore treated with Cymevene from day 74, but did not respond, and as resistance to ganciclovir was suspected the patient was switched to Foscavir therapy on day 87. Ganciclovir resistance was indeed verified subsequently. The high CMV viral loads were successfully suppressed by the

Table 1  
CMV DNA load in QCMD CMV panel 2002 and 2003 measured by ReSSQ<sup>®</sup> CMV Assay

Sample number	Copies/ml		QCMD-ReSSQ Diff Log
	QCMD	ReSSQ	
CMV2002-2	6400	13 600	-0.3
CMV2002-12	6400	9200	-0.2
CMV2002-6	5000	3200	0.1
CMV2002-8	1600	600	0.4
CMV2002-4	1250	1000	0.1
CMV2002-1	400	1240	-0.5
CMV2002-10	400	800	-0.3
CMV2002-11	313	392	-0.1
CMV2002-3	100 (±)	Negative	
CMV2002-9	78 (±)	Negative	
CMV2002-5	Negative	Negative	
CMV2002-7	Negative	Negative	
CMV2003-3	31 250	14 200	0.3
CMV2003-10	31 250	20 700	0.2
CMV2003-5	6250	3020	0.3
CMV2003-12	6250	3550	0.2
CMV2003-4	1250	331	0.6
CMV2003-1	1250	654	0.3
CMV2003-2	250	145	0.2
CMV2003-7	250	113	0.3
CMV2003-9	50 (±)	60	-0.1
CMV2003-11	50 (±)	Negative	
CMV2003-6	Negative	Negative	
CMV2003-8	Negative	Negative	

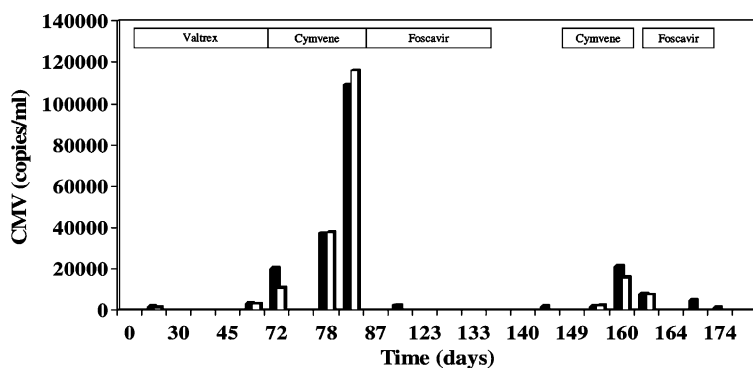


Fig. 4. CMV DNA load change obtained by the COBAS AMPLICOR CMV assay (black) and the ReSSQ CMV<sup>®</sup> Assay (white) in an allogeneic bone marrow-transplant patient who had received Valtrex, Cymvene and Foscavir therapy. Boxes indicate the time period of antiviral therapy. For clarity, the time axis is not drawn to scale.

Foscavir therapy, but as the drug was not well tolerated by the patient, therapy was interrupted. Increasing levels of CMV was again detected at day 153 by both assays,

and suppressed after a second Foscavir treatment. The course of events is clearly reflected in the viral load determinations and both methods yield closely similar results. This shows that the ReSSQ<sup>®</sup> assay is a highly useful tool for CMV viral load monitoring (Zweyberg Wirgart et al., 2005).

#### 4. Diagnosing SARS coronavirus with LightUp<sup>®</sup> probes

Severe acute respiratory syndrome coronavirus (SARS-CoV), is an enveloped, single-stranded, positive-sense RNA virus that belongs to the family *Coronaviridae* (Drosten et al., 2003; Rota et al., 2003). It was first identified during the fall of 2002 in the Guangdong Province in China and the epidemic of SARS in 2003 has affected 30 countries, with 8098 cases and 774 death reported (Liu, 2005). The severity of the disease combined with its rapid spread and lack of specific treatment requires the development of fast and sensitive diagnostic assay (Donnelly et al., 2003).

A ReSSQ<sup>®</sup> assay was developed for detection of specific SARS-CoV genes. This assay was used in collaboration with Swedish Institute for infectious disease control to investigate if nitric oxide (NO) inhibits the replication cycle of SARS-CoV (Åkerström et al., 2005). Nitric oxide is an important signalling molecule between cells and has been shown to have an inhibitory effect on some viruses (Adler et al., 1997; Lane et al., 1997; Pope et al., 1998; Boucher et al., 1999; Coleman, 2001).

To investigate if NO inhibits the viral RNA replication process of SARS-CoV, Vero E6 cells were infected with SARS-CoV at M.O.I 0,1. At 1 h.p.i, the cells were treated with 400  $\mu$ M of the organic NO donor S-Nitroso-*N*-acetylpenicillamine (SNAP) or, as a negative control, with *N*-acetylpenicillamine (NAP), which lacks the NO-donating S-nitroso group, lysed by TRIZOL at different periods of time and total RNA was isolated. The viral RNA was subsequently quantified by Real-time PCR using the ReSSQ<sup>®</sup> SARS assay (LightUp, Technologies AB, Stockholm, Sweden) on a LightCycler 1.0 instrument (Roche Diagnostics, Basel, Switzerland). Quantified armored SARS RNA (CoV-NC), containing the nucleocapsid gene, from Ambion diagnostics was used as a quantification standard (Emery et al., 2004). RNA was used to synthesize cDNA with the SuperScript III RNase H-reverse transcriptase system.

The ReSSQ<sup>®</sup> SARS assay have been used in Fig. 5 to amplify and detect a sequential dilution from 0.5 to 25000 copies/PCR of the Ambion armored RNA standard. It can be seen that all three replicates at the 0.5 copies/PCR level are readily detected which illustrates the excellent sensitivity of the assay. Furthermore, when a standard curve is calculated from the dilution data the PCR efficiency calculated from the slope of the standard curve is close to 100% (Fig. 5).

The specificity of the assay was further investigated by using extracted RNA from several viruses known to cause similar clinical symptoms as template. From the results displayed in Fig. 6 it can be concluded that the ReSSQ<sup>®</sup> SARS assay does not cross-react with any of the tested viruses.

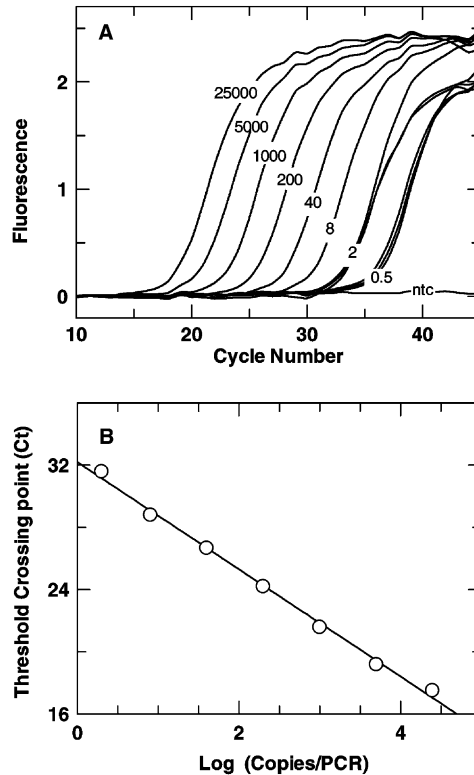


Fig. 5. Sensitivity of a LightUp probe system SARS-CoV NC. (A) Detection of the quantitation standards (SARS-CoV NC, Ambion). The copy number (copies/PCR) are indicated, NTC is the non-template control (negative control). (B) Standard curve: slope  $-3.465$  and intercept  $32.2$ .

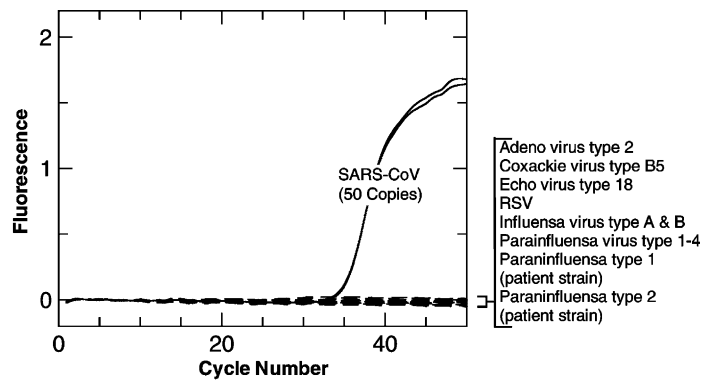


Fig. 6. Specificity of the ReSSQ<sup>®</sup> SARS assay. The specificity was tested against viral RNA of the types indicated. Fifty copies of SARS corona virus were used as positive control.



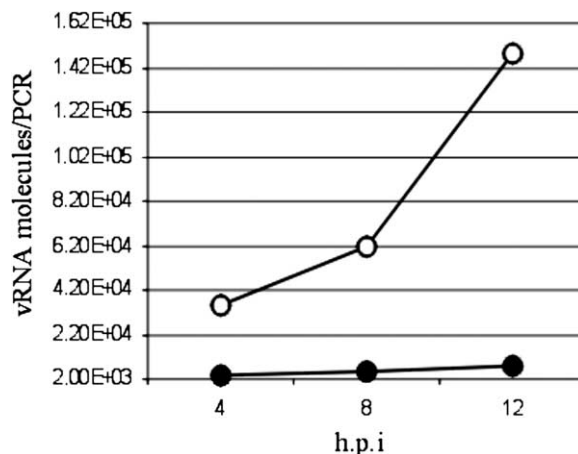


Fig. 7. SNAP blocks the viral RNA replication of SARS-CoV. The Vero E6 cells were infected at an M.O.I. of 0.1 and treated with 400  $\mu$ M SNAP (●) or NAP (○) at 1 h.p.i. Treated cells were lysed by TRIZOL at different periods of time as indicated and the viral RNA quantified as described in the text.

Finally, in Fig. 7 (Reproduced from Akerström et al., 2005) it is shown that 400  $\mu$ M of the NO-donor SNAP significantly inhibits the viral RNA production but that 400  $\mu$ M of NAP has no such effect. This result provides evidence that NO inhibits the SARS Coronavirus and also illustrates the utility of the ReSSQ<sup>®</sup> SARS assay in viral load monitoring of an RNA virus.

## 5. Diagnosing lymphoma with LightUp<sup>®</sup> probes

In most real-time PCR applications disease is monitored by measuring the expression of a marker gene relative to that of a reference gene that is expected to be expressed at a level that is independent of disease state and that is also unaffected by other parameters that may vary among the patients. Today reference genes are selected from optimized reference gene panels such as the Human Endogenous Control Gene Panel from TATAA Biocenter ([www.tataa.com](http://www.tataa.com)). Still, even properly selected reference genes usually show some variation among samples that add to experimental uncertainty in diagnosis. Using the LightUp<sup>®</sup> probes we developed an alternative approach to detect and monitor disease by real-time PCR that does not rely on the stable expression of reference genes (Ståhlberg et al., 2003). Instead of measuring the relative expression of a marker gene to a reference gene, we propose measuring the relative expression of two marker genes that are reciprocally affected by the disease condition. One disease for which this approach is applicable is Non-Hodgkin lymphoma (NHL). NHL develops from the B-lymphocytic lineage and the B-lymphocytes produce immunoglobulins with a heavy chain and either a kappa (IgL $\kappa$ ) or a lambda (IgL $\lambda$ ) light chain (Fig. 8). Each B-lymphocyte decides early in its development which light chain to produce. In healthy humans about 60% of

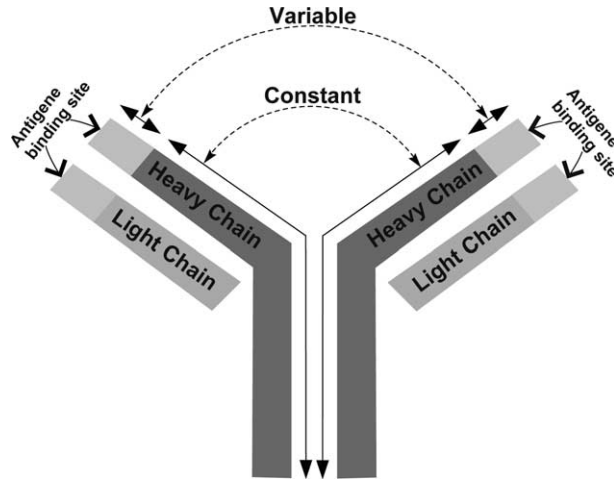


Fig. 8. Schematic drawing of an antibody.

the B-cells produce kappa chains and 40% produce lambda chains. Hence, in normal lymphoid tissue that contains a mixture of B-cells a  $\text{IgL}\kappa:\text{IgL}\lambda$  expression ratio of about 60:40 is expected (Levy et al., 1977). Lymphomas, like all malignant tumors, are clonal and arise from one transformed cell. Lymphoma tissues are dominated by the tumor cells and consequently the  $\text{IgL}\kappa:\text{IgL}\lambda$  ratio is changed. Kappa-producing tumors result in a higher  $\text{IgL}\kappa:\text{IgL}\lambda$  ratio, while lambda-producing tumors result in a lower ratio than 60:40.

### 5.1. Sample preparation

Surgical lymph node biopsies from previously untreated patients were transported from the operation theatre in ice water-chilled boxes and handled in the laboratory within 30 min. Material for the study was rapidly frozen in dry ice/isopentane and stored at  $-70\text{ }^{\circ}\text{C}$ . Fine needle aspirates were suspended in RNAlater (Ambion) directly at the time of sample collection. The cell suspension was stored in RNAlater at  $4\text{ }^{\circ}\text{C}$  for one or two days before the cells were collected by centrifugation and stored frozen at  $-80\text{ }^{\circ}\text{C}$ . Parts of the tissues were fixed in formalin and used for routine diagnostic analysis. Diagnosis was reached by a combination of microscopic evaluation of histology, immunostaining of several markers including those for the kappa and lambda chains (IHC), and in some cases flow cytometry. The samples were classified as lymphadenitis or malignant lymphoma according to the Revised European-American lymphoma (REAL) classification (Harris et al., 1994).

### 5.2. RNA extraction and cDNA analysis

RNA was extracted using the Fast Prep System (FastRNA Green, Qbiogene). Ten micrograms of total RNA was mixed with  $2\text{ }\mu\text{g}$  of pdT oligomers (Pharmacia)

and incubated at 65 °C for 5 min. First strand cDNA synthesis was then performed by adding 0.05 mol/l Tris–HCl, pH 8.3, 0.075 mol/l KCl, 3 mmol/l MgCl<sub>2</sub>, 0.01 mol/l DTT, 10 U/ml M-MLV reverse transcriptase (Life Technologies), 0.05 U/mL RNA guard (Life Technologies) and 10 mmol/l of each deoxyribonucleotide (Life Technologies) to a final volume of 20 µl and incubating the samples at 37 °C for 1 h. The reaction was terminated by incubation at 65 °C for 5 min and samples were stored at –80 °C.

### 5.3. LightUp<sup>®</sup> probes and PCR

Two LightUp probes, H-CCTTTTTCCC-NH<sub>2</sub> (IgLκLUP) and CCTCCTCTCT-NH<sub>2</sub> (IgLλLUP), directed against PCR amplification products of the constant regions in the human immunoglobulin kappa (IgLκ) and lambda (IgLλ) light-chains respectively, were designed. Both probes are homopyrimidine sequences, which are known to exhibit very large signal enhancement upon target binding (Svanvik et al., 2001). Both probes had the thiazole orange derivate, *N*-carboxypentyl-4-[(3'-methyl-1', 3'-benzothiazol-2'-yl) methylenyl] quinolinium iodide as label attached to the peptide nucleic acid. They were synthesized by solid phase synthesis and purified twice by reverse phase HPLC (Svanvik et al., 2000b). Probe concentrations were determined spectroscopically assuming molar absorptivities at 260 nm of 83 100 (mol/l)<sup>-1</sup>cm<sup>-1</sup> for IgLκLUP and 81 100 (mol/l)<sup>-1</sup>cm<sup>-1</sup> for IgLλLUP (Svanvik et al., 2000b). The probes were designed to have melting temperatures of 65–70 °C, which is between the annealing (55 °C) and elongation (74 °C) temperatures of the PCRs. PCR systems were designed for a 231 bp fragment of the human IgLκ (GenBank accession number AK024974) and a 223 bp fragment of the human IgLλ (GenBank accession number X51755) comprising the IgLκLUP and IgLλLUP target sequences, respectively. Reaction conditions were optimized as described elsewhere (Kubista et al., 2001). IgLκ and IgLλ PCR:s both contained 75 mmol/l Tris (pH 8.8), 20 mmol/l (NH<sub>4</sub>)<sub>2</sub>SO<sub>4</sub>, 0.1% Tween 20, 1 U of JumpStart<sup>TM</sup> Taq DNA polymerase (with antibody) (Sigma-Aldrich) and 200 ng/µL of Bovine Serum Albumin (Fermentas). Specific components for the IgLκ PCR were 5 mmol/l MgCl<sub>2</sub>, 0.2 mmol/l deoxyribonucleotides (Sigma-Aldrich), 800 nmol/l of each primer (Med-Probe Inc) and 800 nmol/l IgLκLUP, and for the IgLλ PCR 3.5 mmol/l MgCl<sub>2</sub>, 0.4 mmol/l deoxyribonucleotides, 600 nmol/l of each primer and 600 nmol/l IgLλLUP. Primer sequences were for IgLκ 5'-TGA GCA AAG CAG ACT ACG AGA-3' (forward) and 5'-GGG GTG AGG TGA AAG ATG AG-3' (reverse), and for IgLλ 5'-GAG CCT GAC GCC TGA G-3' (forward) and 5'-ATT GAG GGT TTA TTG AGT GCA G-3' (reverse).

Real-time PCR was measured in a LightCycler (Roche Diagnostics) using the thermocycler program: 3 min pre-incubation at 95 °C followed by 50 cycles for 0 s at 95 °C, 10 s at 55 °C and 11 s at 74 °C. Fluorescence was monitored at the end of the annealing phase using 470 nm excitation and 530 nm emission (the LightCycler F1 channel). All amplification curves were baseline adjusted by subtracting the arithmetic average of the five lowest fluorescence read-out values in each sample (arithmetic baseline adjustment in the LightCycler software). The threshold was set

to a value of 1.00, which was significantly above background noise, and the number of cycles required to reach this level,  $C_t$ , was determined.

#### 5.4. Classification of patient samples

Thirty-two patient samples were analyzed for B-cell lymphoma by the LightUp Q-PCR assays. Twenty samples were surgical biopsies and 12 were collected as fine needle aspirates (Ståhlberg et al., 2003). All samples were run in duplicates including negative controls. The data are presented in Fig. 9. In the scatter plot each symbol represents one sample and is positioned in the plot on the coordinate  $(CT_{IgL\kappa}, CT_{IgL\lambda})$ . The corresponding number of cDNA molecules of purified template is indicated in logarithmic scale on the opposite axes. Samples found negative by IHC analysis are shown in green and positive samples are shown in red. The samples above the pink arc are those collected as fine needle aspirates. The relative expression of two genes is given by (Ståhlberg et al., 2005):

$$\frac{N_{0_{IgL\kappa}}}{N_{0_{IgL\lambda}}} = K_{RS} * \frac{\eta_{IgL\lambda}(1 + E_{IgL\lambda})^{CT_{IgL\lambda}-1}}{\eta_{IgL\kappa}(1 + E_{IgL\kappa})^{CT_{IgL\kappa}-1}} \quad (1)$$

This can be rearranged into linear form (Ståhlberg et al., 2003):

$$CT_{IgL\kappa} = b * CT_{IgL\lambda} + m \quad (2)$$

Hence, the data points representing negative samples in the scatter plot can be fitted to a straight line that will represent the  $IgL\kappa:IgL\lambda$  expression ratio of healthy indi-

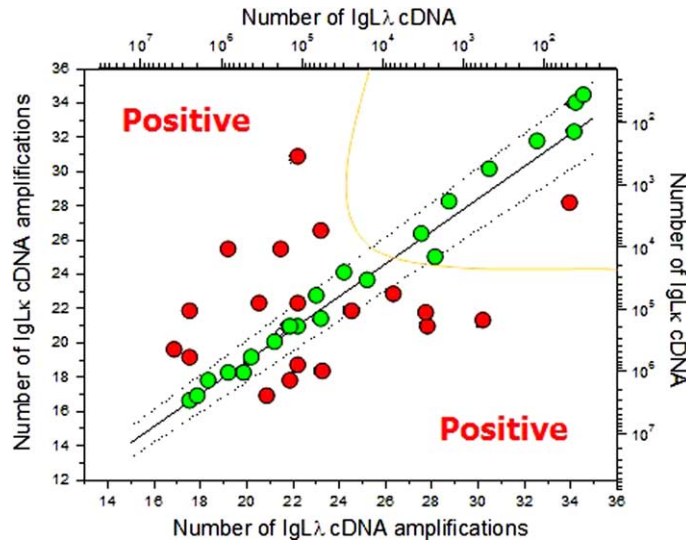


Fig. 9. Scatter plot of the expression of the  $\kappa$  and  $\lambda$  immunoglobulin light chain genes in patient samples. Samples classified as NHL positive by REAL are shown in red, while negative samples are shown in green. The solid line reflects 60:40  $IgL\kappa:IgL\lambda$  expression ratio. The dotted lines indicate 95% confidence interval of negative samples. Samples within the pink arc were collected as fine needle aspirates.

viduals. The approach does not require the  $\text{IgL}\kappa:\text{IgL}\lambda$  expression ratio to be known. In fact, the estimated ratio of 60:40 is for the  $\text{IgL}\kappa:\text{IgL}\lambda$  light chains, which is the ratio of the protein products. The ratio of the corresponding mRNAs could be different, for example, due to a difference in translation efficiencies of the mRNAs. In the original study the authors estimated the parameters in Eq. (1) from a detailed characterization of a subset of the samples by in situ calibration (Ståhlberg et al., 2003). They found that the  $\text{IgL}\kappa:\text{IgL}\lambda$  mRNA expression ratio of negative samples indeed is close to 60:40, and the authors could also calculate 95% confidence interval for the negative samples. The confidence interval is indicated in the scatter plot by the dashed lines. Hence, negative samples based on QPCR results are expected to be within the dashed lines, while positive samples with  $\kappa$  clonality are found below the lines and samples with  $\lambda$  clonality are above the lines. The agreement between the QPCR (position in the scatter plot) and IHC (color) classifications is excellent. For the fine needle aspirates, found above the arc in Fig. 9, the agreement was perfect, even though these samples contained very few cells and therefore not very much mRNA. This very high predictive power of the LightUp probed  $\text{IgL}\kappa$  vs.  $\text{IgL}\lambda$  assay demonstrates the strength of designing assays based on relative expression of two reciprocal marker genes instead of comparing expression of a single marker gene with that of a reference gene. Recently, the same strategy was used to diagnose mantle cell lymphoma by measuring the  $CCND1:CCND3$  expression ratio (Jones et al., 2004). The strategy is not limited to two marker genes. Any number of marker genes can be used, and companies such as MultiD Analyses ([www.multid.se](http://www.multid.se)) are developing software to classify samples based on an arbitrary number of marker genes, without relying on reference genes, by identifying characteristic expression patterns.

## 6. Conclusions

The LightUp<sup>®</sup> probe technology has been shown to be useful for monitoring viral loads both of DNA virus such as the cytomegalovirus and RNA viruses such as the SARS corona virus. The effects of antiviral treatment and nitric oxide are readily detected. It is noteworthy that LightUp<sup>®</sup> probes are short, typically 8–12 residues, which is very useful in viral diagnostics where the mutation frequency often is high and long conserved regions may be rare. This is particularly true for RNA viruses such as HIV, Influenza and SARS.

A LightUp probe assay has also been shown to quantify the relative expression of the kappa/lambda genes in a way that allows diagnosis of B-lymphocyte monoclonality.

## References

- Adler, H., Beland, J.L., Del-Pan, N.C., Kobzik, L., Brewer, J.P., Martin, T.R., Rimm, I.J., 1997. Suppression of herpes simplex virus type 1 (HSV-1)-induced pneumonia in mice by inhibition of inducible nitric oxide synthase (iNOS, NOS2). *J. Exp. Med.* 185, 1533–1540.

- Afonina, I., Zivarts, M., Kutuyavin, I., Lukhtanov, E., Gamper, H., Meyer, R.B., 1997. Efficient priming of PCR with short oligonucleotides conjugated to a minor groove binder. *Nucleic Acids Res.* 25, 2657–2660.
- Akerström, S., Mousavi-Jazi, M., Klingström, J., Leijon, M., Lundkvist, A., Mirazimi, A., 2005. Nitric oxide inhibits the replication cycle of severe acute respiratory syndrome coronavirus. *J. Virol.* 79, 1966–1969.
- Bernard, P.S., Lay, M.J., Wittwer, C.T., 1998. Integrated amplification and detection of the C677T point mutation in the methylenetetrahydrofolate reductase gene by fluorescence resonance energy transfer and probe melting curves. *Anal. Biochem.* 255, 101–107.
- Boucher, J.L., Moali, C., Tenu, J.P., 1999. Nitric oxide biosynthesis, nitric oxide synthase inhibitors and arginase competition for L-arginine utilization. *Cell. Mol. Life Sci.* 55, 1015–1028.
- Coleman, J.W., 2001. Nitric oxide in immunity and inflammation. *Int. Immunopharmacol.* 1, 1397–1406.
- Demidov, V.V., Potaman, V.N., Frank-Kamenetskii, M.D., Egholm, M., Buchard, O., Sönnichsen, S.H., Nielsen, P.E., 1994. Stability of peptide nucleic acids in human serum and cellular extracts. *Biochem. Pharmacol.* 48, 1310–1313.
- Donnelly, C.A., Ghani, A.C., Leung, G.M., Hedley, A.J., Fraser, C., Riley, S., Abu-Raddad, L.J., Ho, L.M., Thach, T.Q., Chau, P., Chan, K.P., Lam, T.H., Tse, L.Y., Tsang, T., Liu, S.H., Kong, J.H., Lau, E.M., Ferguson, N.M., Anderson, R.M., 2003. Epidemiological determinants of spread of causal agent of severe acute respiratory syndrome in Hong Kong. *Lancet* 361, 1761–1766.
- Drosten, C., Günther, S., Preiser, W., van der Werf, S., Brodt, H.R., Becker, S., Rabenau, H., Panning, M., Kolesnikova, L., Fouchier, R.A., Berger, A., Burguière, A.M., Cinatl, J., Eickmann, M., Escriou, N., Grywna, K., Kramme, S., Manuguerra, J.C., Müller, S., Rickerts, V., Stürmer, M., Vieth, S., Klenk, H.D., Osterhaus, A.D., Schmitz, H., Doerr, H.W., 2003. Identification of a novel coronavirus in patients with severe acute respiratory syndrome. *N. Engl. J. Med.* 348, 1967–1976.
- Egholm, M., Buchardt, O., Christensen, L., Behrens, C., Freier, S.M., Driver, D.A., Berg, R.H., Kim, S.K., Norden, B., Nielsen, P.E., 1993. PNA hybridizes to complementary oligonucleotides obeying the Watson–Crick hydrogen-bonding rules. *Nature* 365, 566–568.
- Emery, S.L., Erdman, D.D., Bowen, M.D., Newton, B.R., Winchell, J.M., Meyer, R.F., Tong, S., Cook, B.T., Holloway, B.P., McCaustland, K.A., Rota, P.A., Bankamp, B., Lowe, L.E., Ksiazek, T.G., Bellini, W.J., Anderson, L.J., 2004. Real-time reverse transcription-polymerase chain reaction assay for SARS-associated coronavirus. *Emerg. Infect. Dis.* 10, 311–316.
- Fafi-Kremer, S., Brengel-Pesce, K., Barguès, G., Bourgeat, M.J., Genoulaz, O., Seigneurin, J.M., Morand, P., 2004. Assessment of automated DNA extraction coupled with real-time PCR for measuring Epstein-Barr virus load in whole blood, peripheral mononuclear cells and plasma. *J. Clin. Virol.* 30, 157–164.
- Foy, C.A., Parkes, H.C., 2001. Emerging homogeneous DNA-based technologies in the clinical laboratory. *Clin. Chem.* 47, 990–1000.
- Harris, N.L., Jaffe, E.S., Stein, H., Banks, P.M., Chan, J.K., Cleary, M.L., Delsol, G., De Wolf-Peeters, C., Falini, B., Gatter, K.C., 1994. A revised European-American classification of lymphoid neoplasms: a proposal from the International Lymphoma Study Group. *Blood* 84, 1361–1392.
- Herrmann, B., Larsson, V.C., Rubin, C.J., Sund, F., Eriksson, B.M., Arvidson, J., Yun, Z., Bondeson, K., Blomberg, J., 2004. Comparison of a duplex quantitative real-time PCR assay and the COBAS Amplicor CMV Monitor test for detection of cytomegalovirus. *J. Clin. Microbiol.* 42, 1909–1914.
- Jones, C.D., Darnell, K.H., Warnke, R.A., Zehnder, J.L., 2004. CyclinD1/CyclinD3 ratio by real-time PCR improves specificity for the diagnosis of mantle cell lymphoma. *J. Mol. Diagn.* 6, 84–89.
- Kalpole, J.S., Schippers, E.F., Eling, Y., Sijpkens, Y.W., de Fijter, J.W., Kroes, A.C., 2005. Similar reduction of cytomegalovirus DNA load by oral valganciclovir and intravenous ganciclovir on pre-emptive therapy after renal and renal-pancreas transplantation. *Antivir. Ther.* 10, 119–123.
- Karlsson, H.J., Bergqvist, M.H., Lincoln, P., Westman, G., 2004. Syntheses and DNA-binding studies of a series of unsymmetrical cyanine dyes: structural influence on the degree of minor groove binding to natural DNA. *Bioorg. Med. Chem.* 12, 2369–2384.
- Karlsson, H.J., Eriksson, M., Perzon, E., Akerman, B., Lincoln, P., Westman, G., 2003. Groove-binding unsymmetrical cyanine dyes for staining of DNA: syntheses and characterization of the DNA-binding. *Nucleic Acids Res.* 31, 6227–6234.

- Kubista, M., Ståhlberg, A., Bar, T., 2001. Light-up probe based real-time Q-PCR. In: Raghavachari, R., Tan, W. (Eds.), *Genomics and Proteomics Technologies*. Proceedings of SPIE, vol. 4264. International Society of Optical Engineering, Bellingham, WA, pp. 53–58.
- Lane, T.E., Paoletti, A.D., Buchmeier, M.J., 1997. Disassociation between the in vitro and in vivo effects of nitric oxide on a neurotropic murine coronavirus. *J. Virol.* 71, 2202–2210.
- Leijon, M., 2004. LightUp Probes. In: Fuchs, J., Podda, M. (Eds.), *Encyclopedia of Diagnostic Genomics and Proteomics*. Marcel Dekker Inc, New York, pp. 718–720.
- Levy, R., Warnke, R., Dorfman, R.F., Haimovich, J., 1977. The monoclonality of human B-cell lymphomas. *J. Exp. Med.* 145, 1014–1028.
- Liu, W., 2005. Molecular Epidemiology of SARS-associated Coronavirus, Beijing. *Emerg. Infect. Dis.* 11, 1420–1424.
- Livak, K.J., Flood, S.J., Marmaro, J., Giusti, W., Deetz, K., 1995. Oligonucleotides with fluorescent dyes at opposite ends provide a quenched probe system useful for detecting PCR product and nucleic acid hybridization. *PCR Methods Appl.* 4, 357–362.
- Mackay, I.M., 2004. Real-time PCR in the microbiology laboratory. *Clin. Microbiol. Infection* 10, 190–212.
- Mackay, I.M., Arden, K.E., Nitsche, A., 2002. Real-time PCR in virology. *Nucleic Acids Res.* 30, 1292–1305.
- Mengoli, C., Cusinato, R., Biasolo, M.A., Cesaro, S., Parolin, C., Palù, G., 2004. Assessment of CMV load in solid organ transplant recipients by pp65 antigenemia and real-time quantitative DNA PCR assay: correlation with pp67 RNA detection. *J. Med. Virol.* 74, 78–84.
- Nielsen, P.E., Egholm, M., Berg, R.H., Buchardt, O., 1991. Sequence-selective recognition of DNA by strand displacement with a thymine-substituted polyamide. *Science* 254, 1497–1500.
- Nye, M.B., Leman, A.R., Meyer, M.E., Menegus, M.A., Rothberg, P.G., 2005. Sequence diversity in the glycoprotein B gene complicates real-time PCR assays for detection and quantification of cytomegalovirus. *J. Clin. Microbiol.* 43, 4968–4971.
- Pope, M., Marsden, P.A., Cole, E., Sloan, S., Fung, L.S., Ning, Q., Ding, J.W., Leibowitz, J.L., Phillips, M.J., Levy, G.A., 1998. Resistance to murine hepatitis virus strain 3 is dependent on production of nitric oxide. *J. Virol.* 72, 7084–7090.
- Rota, P.A., Oberste, M.S., Monroe, S.S., Nix, W.A., Campagnoli, R., Icenogle, J.P., Peñaranda, S., Bankamp, B., Maher, K., Chen, M.H., Tong, S., Tamin, A., Lowe, L., Frace, M., DeRisi, J.L., Chen, Q., Wang, D., Erdman, D.D., Peret, T.C., Burns, C., Ksiazek, T.G., Rollin, P.E., Sanchez, A., Liffick, S., Holloway, B., Limor, J., McCaustland, K., Olsen-Rasmussen, M., Fouchier, R., Günther, S., Osterhaus, A.D., Drosten, C., Pallansch, M.A., Anderson, L.J., Bellini, W.J., 2003. Characterization of a novel coronavirus associated with severe acute respiratory syndrome. *Science* 300, 1394–1399.
- Schuurman, T., van Breda, A., de Boer, R., Kooistra-Smid, M., Beld, M., Savelkoul, P., Boom, R., 2005. Reduced PCR sensitivity due to impaired DNA recovery with the MagNA Pure LC total nucleic acid isolation kit. *J. Clin. Microbiol.* 43, 4616–4622.
- Spector, S.A., Hsia, K., Crager, M., Pilcher, M., Cabral, S., Stempien, M.J., 1999. Cytomegalovirus (CMV) DNA load is an independent predictor of CMV disease and survival in advanced AIDS. *J. Virol.* 73, 7027–7030.
- Spector, S.A., Wong, R., Hsia, K., Pilcher, M., Stempien, M.J., 1998. Plasma cytomegalovirus (CMV) DNA load predicts CMV disease and survival in AIDS patients. *J. Clin. Invest.* 101, 497–502.
- Ståhlberg, A., Aman, P., Ridell, B., Mostad, P., Kubista, M., 2003. Quantitative real-time PCR method for detection of B-lymphocyte monoclonality by comparison of kappa and lambda immunoglobulin light chain expression. *Clin. Chem.* 49, 51–59.
- Ståhlberg, A., Zoric, N., Aman, P., Kubista, M., 2005. Quantitative real-time PCR for cancer detection: the lymphoma case. *Expert. Rev. Mol. Diagn.* 5, 221–230.
- Svanvik, N., Nygren, J., Westman, G., Kubista, M., 2001. Free-probe fluorescence of light-up probes. *J. Am. Chem. Soc.* 123, 803–809.
- Svanvik, N., Ståhlberg, A., Sehlstedt, U., Sjöback, R., Kubista, M., 2000a. Detection of PCR products in real time using light-up probes. *Anal. Biochem.* 287, 179–182.

- Svanvik, N., Westman, G., Wang, D., Kubista, M., 2000b. Light-up probes: thiazole orange-conjugated peptide nucleic acid for detection of target nucleic acid in homogeneous solution. *Anal. Biochem.* 281, 26–35.
- Tanaka-Kitajima, N., Sugaya, N., Futatani, T., Kanegane, H., Suzuki, C., Oshiro, M., Hayakawa, M., Futamura, M., Morishima, T., Kimura, H., 2005. Ganciclovir therapy for congenital cytomegalovirus infection in six infants. *Pediatr. Infect. Dis. J.* 24, 782–785.
- Tyagi, S., Kramer, F.R., 1996. Molecular beacons: probes that fluoresce upon hybridization. *Nat. Biotechnol.* 14, 303–308.
- Uhl, J.R., Vetter, E.A., Boldt, K.L., Johnston, B.W., Ramin, K.D., Adams, M.J., Ferrieri, P., Reischl, U., Cockerill, F.R., 2005. Use of the Roche LightCycler Strep B assay for detection of group B *Streptococcus* from vaginal and rectal swabs. *J. Clin. Microbiol.* 43, 4046–4051.
- Wallace, P.S., 2003. Linkage between the journal and Quality Control Molecular Diagnostics (QCMD). *J. Clin. Virol.* 27, 211–212.
- Zweyberg Wirgart, B., Andersson, P., Grillner, L., 2005. Evaluation of the ReSSQ assay in relation to the COBAS AMPLICOR CMV MONITOR test and an in-house nested PCR method for detection of cytomegalovirus DNA. *J. Clin. Microbiol.* 43, 4057–4063.